Investigation on the radiated EMI of a 3-phase traction inverter for urban mobility

Filippo Pellitteri, Nicola Campagna, Massimo Caruso, Antonino Oscar Di Tommaso, Gerlando Frequente and Rosario Miceli
Dept. of Engineering
University of Palermo
Palermo, Italy
filippo.pellitteri@unipa.it, nicola.campagna@unipa.it, massimo.caruso16@unipa.it, antoninooscar.ditommaso@unipa.it, gerlando.frequente@unipa.it, rosario.miceli@unipa.it

Annalisa Contato
Dept. of Architecture
University of Palermo
Palermo, Italy
annalisa.contato@unipa.it,

Geraldina Signa
Dept. of of Earth and Marine Sciences
University of Palermo
Palermo, Italy
geraldina.signa@unipa.it

***Abstract*— In synergy with the European Green Deal, which aims at providing direct support for cities to strive for climate neutrality, the search for innovative energy production, storage, conversion and utilization solutions to be applied in the context of mobility is becoming increasingly important to meet the needs for energy savings, risk reduction and ecological footprint while ensuring equity, inclusiveness and sustainable use of goods and services. As far as conversion systems are concerned, for the purpose of higher and higher levels of transportation electrification, power converters based on emerging semiconductor technologies of switching devices, such as wide bandgap (WGB) devices, are essential to efficiently guarantee high voltage levels while operating at high frequencies. Moreover, alternative topologies of connections among switching devices are currently investigated to further support power converters' performances. Nevertheless, high-frequency high-voltage switching power converters are implemented at the price of high electromagnetic interference (EMI) noises, so that limiting the radiated EMI of such power converters is a must. In this paper, a 3-phase traction inverter based on Silicon Carbide (SiC) devices connected through cascode configuration is proposed. A 600 V prototype has been assembled and experimentally tested, also regarding its radiated EMI, measured inside a semi-anechoic chamber.**

Keywords—radiated EMI, traction inverter, SiC devices, power converters, power modules, three phase motor drive.

I. INTRODUCTION

In the recent years, power electronics has increasingly used Wide bandgap (WBG) semiconductor switching devices, due to better performances in terms of high switching frequencies and voltage levels with respect to the traditional Silicon (Si) devices.

Silicon Carbide (SiC) features different properties that make it a better semiconductor material if compared to Si, such as higher values of bandgap energy, breakdown field, saturation electron velocity and thermal conductivity [1]. These attractive features provide SiC with better performances in terms of switching characteristics [2] and thermal properties [3].

Due to the afore-mentioned advantages and to the last technological developments, SiC has been playing a key role to push power converters towards increasingly high switching frequencies and voltage levels, keeping high reliability and low power losses in several applications, including electrical mobility, bringing to power converters a significant contribution concerning efficiency, power density and high temperature operations. [4-7].

While importance of SiC diodes due to their null reverse recovery charge is well-known since long time, SiC transistors have great developments margins, especially according to the different technologies which can be exploited for different applications. Regarding this, SiC MOSFETs are substantially drivable as the corresponding Si ones, with the benefit of better performances at the highest voltage levels, so that SiC MOSFETs are good candidates to replace Si IGBTs.

As far as Gallium Nitride (GaN) electronic switching devices are concerned, they enable high efficiency and small passive components, thus allowing to obtain higher power density if compared to Si-based electrical systems. Nevertheless, with respect to SiC ones, GaN devices are rated for lower voltage levels: while SiC devices are strongly recommended for more than 1000 V, GaN devices are more performant for maximum 650 V. Regarding the electron mobility, GaN shows much higher values than both Si and SiC, thus allowing for notably high switching frequencies [8]. Thermal conductivity, costs and reliability are still some aspects that address the choice towards SiC, as far as high-voltage mobility applications are concerned [9].

Considering SiC devices more in detail, SiC JFET provide even better performances than SiC MOSFETs, but they require a careful gate driving, especially normally-on transistors. Therefore, a trade-off solution is desirable, collecting the benefits of an easy drivability and of high conductivity and low switching transients. This convenient combination can be implemented by the cascode connection, which is the series connection between a low-voltage switching pilot device, driven by an external signal, and a high-voltage device which is driven according to the state of the first one. These two devices are generally corresponding to a normally-off low-voltage switch and a normally-on high-voltage switch respectively [10-12].

The combination between SiC material and cascode connection is therefore recommended to achieve reliable results: the pilot normally-off device can be realized through a SiC MOSFET, whereas the self-driven normally-on is well implemented by a SiC JFET. The SiC MOSFET gives a notable contribution in terms of speed of the switching transient with respect to a low voltage Silicon MOSFET, due to the small gate-source capacitance and to the fast body-diode, which allows to properly turn-on into reverse conduction: due to the reverse current flowing through the body-diode, which is connected between gate and source of the JFET, the high-voltage device is turned-on. The self-driven device is implemented through a SiC FET, which is more reliable in terms of thermal management with respect to a GaN device and therefore it is more performant as high-voltage device. A background on state-of-art SiC JFET devices and their applications is provided in [13-16].

The promising performances of SiC cascode configuration in terms of fast switching transients are obtained at the price of high frequency EMI noises. Indeed, with the higher and higher levels of dV/dt guaranteed by WBG devices with respect to conventional Si devices and by cascode connection with respect to the single switch, EMI noises are increasingly higher in amplitude and at higher frequencies. Limiting the radiated EMI is therefore essential to make the use of WBG devices, as well as cascode connection, really convenient for several application fields, including sustainable mobility. Regarding this, power electronics plays a crucial role as well as electrical drives and energy storage systems [17-20].

Due to their influence on the noise emitted by the power module, modeling the parasitic elements of the PCB can be crucial to foresee the switching transients of the voltage waveforms and therefore the radiated EMI as well. Indeed, by implementing the FFT on the simulated voltage waveforms of the converter, it is possible to evaluate the noise emitted by the unintentional antennas of the system, represented by the terminal cables. By the combination between the emitted noise and the gain factor of the receiving antenna, which depends on the frequency, it should be possible to obtain the radiated electric field and to relate it to the modelled parasitic elements, thus aiming at a way to minimizing them.

In this paper, a cascode-based 3-phase traction inverter implemented through SiC MOSFETs as pilot devices and SiC JFETs as self-driven devices is proposed. A PCB prototype has been realized and experimental tests have proven its correct operation for a 3-phase induction motor power supply. To evaluate the radiated EMI and its dependance on the parasitic elements of the power module, the experimental results in terms of radiated electric field have been related to the simulation ones, carried out considering the equivalent PCB tracks inductances of the power converter.

Simulation results concerning the switching transients, main responsible of the emitted noise, have been compared to those without considering parasitic inductances, thus aiming at understanding their influence on the EMI noise.

The experimental tests have been reproduced inside a semi-anechoic chamber.

II. SiC CASCODE CONFIGURATION

The proposed solution of SiC-based cascode configuration consists of an enhancement n-channel MOSFET used as pilot device and a n-channel JFET as high-voltage device.

This JFET is a normally-on device, due to its negative threshold gate-source voltage The direct connection between the MOSFET source and the JFET gate nodes makes this switching configuration totally self-driven, since when the MOSFET is on, the gate-source voltage of the JFET is zero and therefore the JFET is on as well.

The SiC-based MOSFET-JFET cascode combination is proposed as single element of the six switches implementing a 3-phase inverter, as highlighted in Fig. 1.

A prototype of the proposed cascode-based 3-phase inverter has been assembled to evaluate its proper working, according to appropriate layout design criteria, aiming at high frequency noise reduction and at avoiding electrical arcs according to the rated voltage levels.

Furthermore, ground paths are separated from ground plane concerning the paths with high di/dt.

A detail of the proposed layout is proposed in Fig. 2, highlighting a 2-layer PCB scheme.

As far as the produced radiated EMI, this shall be carefully investigated to understand the role of high dV/dt, meaning high voltage levels and short switching transients. Even aiming at smoothing radiated EMI through stray inductances minimization and proper positioning of electronic components on the printed circuit board (PCB), the cables at the terminal sections of the switching power conveter can act as unintentional antennas.

Moreover, the equivalent track inductances should be modeled to determine their influence on the EMI noise. The related experimental prototype is shown in Fig. 3.

Some of the performed experimental results concerning the operation of the cascode SiC converter supplying a 3-phase induction machine are shown in Fig. 4, for a 250 V DC-link voltage. Due to limitations in the voltage range of the available DC power source, higher voltage levels have not been tested yet, even though the used SiC JFET device voltage rating is 1200 V. Modulation and carrier frequency concerning the implemented three-phase sinusoidal PWM are 50 Hz and 40 kHz respectively.

The rise voltage of one of the cascode-based switches is shown, corresponding to a dV/dt equal to about 5 V/ns.

The significance of the dV/dt is related to the produced radiated EMI.

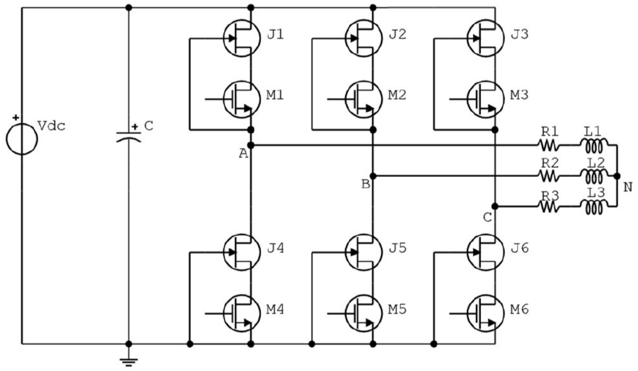

Fig. 1 Schematic of the 3-phase inverter based on nMOS/JFET cascode with SiC devices.

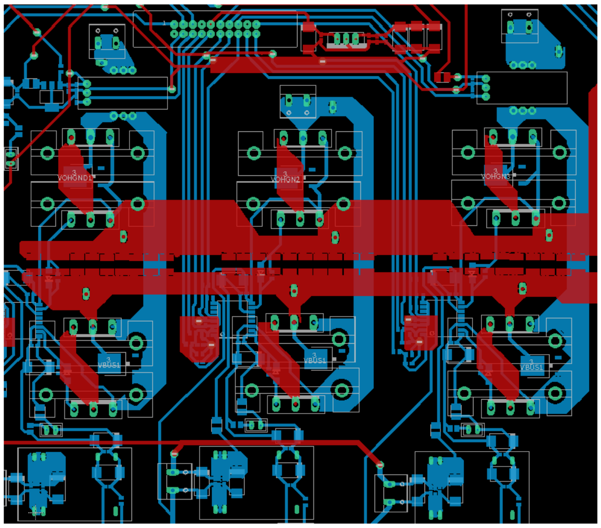

Fig. 2 Layout design of the proposed 3-phase inverter.

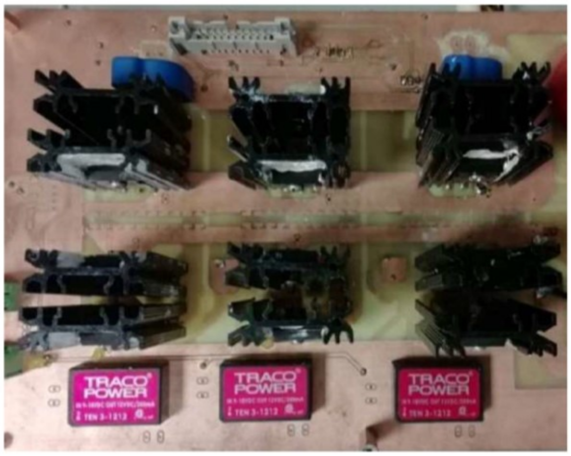

Fig. 3 Top view of the experimental prototype of the proposed 3-phase inverter.

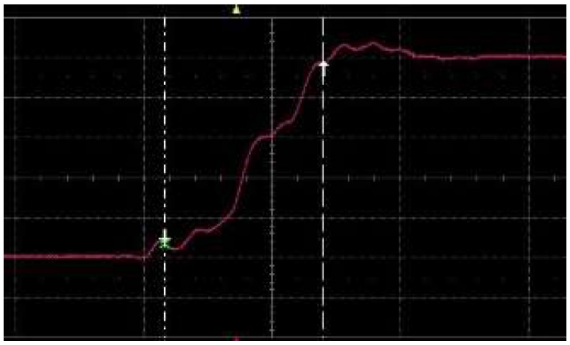

Fig. 4 Rise time of a cascode voltage during a switching transient; voltage division: 150 V/div; time division: 30 ns/div.

III. RADIATED EMI OF THE PROPOSED CONVERTER

The realized SiC cascode 3-phase inverter is supposed to be experimentally tested also regarding its radiated EMI, through measurements inside a semi-anechoic chamber.

Fig. 5 shows the block diagram related to the experimental setup for the radiated EMI measurements implementation: the device under test (DUT) radiates emissions towards an antenna, which is connected to the EMI receiver. The LabVIEW Virtual Instrument block processes the EMI receiver results, consisting in the achieved spectrum, splitting them into horizontal and vertical polarization.

Fig. 6 shows the correspondent setup schematic considering it in a semi-anechoic chamber.

The achieved results for a 250 V DC-link voltage are shown in Figures 7 and 8, corresponding to vertical and horizontal polarization respectively. Limits imposed by the International Special Committee On Radio Interference (CISPR) are highlighted as well. More in detail, Product Standards CISPR 12 and CISPR 25 should be considered to address protection of off-board and on-board receivers from EMI concerning vehicles and boats [21].

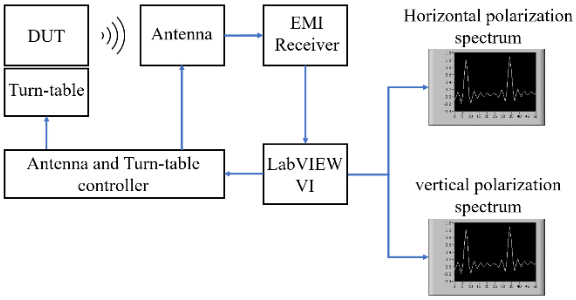

Fig. 5 Diagram of the radiated EMI measurements setup..

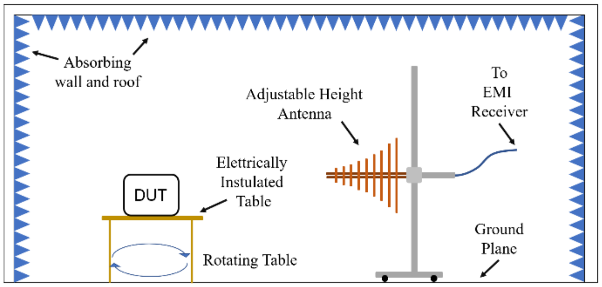

Fig. 6 Radiated EMI measurements setup in semi-anechoic chamber.

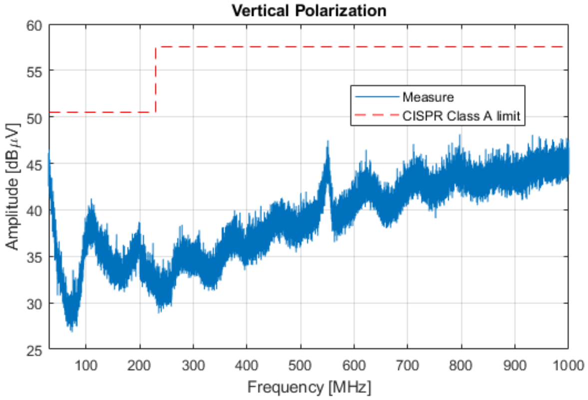

Fig.7 Measured radiated EMI vs. frequency: vertical polarization.

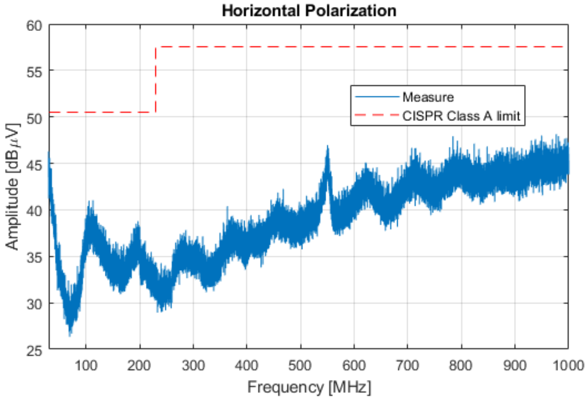

Fig. 8 Measured radiated EMI vs. frequency: horizontal polarization.

IV. CONCLUSIONS

In this paper, a 3-phase cascode-based inverter implemented through SiC devices has been proposed. The assembled experimental prototype has been tested, aiming at the demonstration of its proper operation.

Results regarding the obtained waveforms have been addressed for a voltage level of 250 V, concerning the DC-link supplying the 3-phase inverter. Tested power rating of the inverter is 100 W, even if in future tests the goal power level will be 1 kW.

Moreover, the measurements about radiated EMI, exploiting the availability of a semi-anechoic chamber, have been performed and referred to the existing standards related to mobility sector.

Future developments of the presented work imply the implementation of a closed-loop control strategy on the power converter and the extension of the tested voltage range until 1000 V to evaluate the reliability of the employed devices in the framework of the proposed topology.

ACKNOWLEDGMENT

This work was realized with the contribution of: PON R&I 2014-2020 (PON R&I FSE-REACT EU), Azione IV.6 “Contratti di ricerca su tematiche Green” to fund and support the research; research project “Sustainable Innovative transport SYstems for MEtropolitan Cities (SISYMEC)”, in the frame of the call EUROSTART from University of Palermo, funded by DM 737/2021 of the Italian Ministry of University and Research; SAMOTHRACE - Sicilian Micro and Nano Technologies Research and Innovation Center - SPOKE 3 S2-COMMs (Micro and Nanotechnologies for Smart & Sustainable Communities).

REFERENCES

[1] P. Vaculik, "The properties of SiC in comparison with Si semiconductor devices," 2013 International Conference on Applied Electronics, Pilsen, Czech Republic, 2013, pp. 1-4.

[2] A. Ong, J. Carr, J. Balda and A. Mantooth, "A Comparison of Silicon and Silicon Carbide MOSFET Switching Characteristics," 2007 IEEE Region 5 Technical Conference, Fayetteville, AR, USA, 2007, pp. 273-277, doi: 10.1109/TPSD.2007.4380318.

[3] R. Kibushi, T. Hatakeyama, K. Yuki, N. Unno and M. Ishizuka, "Comparison of thermal properties between Si and SiC power MOSFET using electro-thermal analysis," 2017 International Conference on Electronics Packaging (ICEP), Yamagata, Japan, 2017, pp. 188-192, doi: 10.23919/ICEP.2017.7939354.

[4] D. Han, J. Noppakunkajorn and B. Sarlioglu, "Efficiency comparison of SiC and Si-based bidirectional DC-DC converters," 2013 IEEE Transportation Electrification Conference and Expo (ITEC), 2013, pp. 1-7, doi: 10.1109/ITEC.2013.6574511

[5] Xun, Qian & Xun, Boyang & Li, Zuxin & Wang, Peiliang & Cai, Zhiduan. (2016). Application of SiC power electronic devices in secondary power source for aircraft. Renewable and Sustainable Energy Reviews. 70. 10.1016/j.rser.2016.12.035.

[6] T. Daranagama, F. Udrea, T. Logan and R. McMahon, "A performance comparison of SiC and Si devices in a bi-directional converter for distributed energy storage systems," 2016 IEEE 7th International Symposium on Power Electronics for Distributed Generation Systems (PEDG), Vancouver, BC, Canada, 2016, pp. 1-8, doi: 10.1109/PEDG.2016.7527041.

[7] D. C. Sheridan, A. Ritenour, R. Kelley, V. Bondarenko and J. B. Casady, "Advances in SiC VJFETs for renewable and high-efficiency power electronics applications," The 2010 International Power Electronics Conference - ECCE ASIA -, 2010, pp. 3254-3258, doi: 10.1109/IPEC.2010.5543703.

[8] N. Keshmiri, D. Wang, B. Agrawal, R. Hou and A. Emadi, "Current Status and Future Trends of GaN HEMTs in Electrified Transportation," in IEEE Access, vol. 8, pp. 70553-70571, 2020, doi: 10.1109/ACCESS.2020.2986972.

[9] G. Su, "Comparison of Si, SiC, and GaN based Isolation Converters for Onboard Charger Applications," 2018 IEEE Energy Conversion Congress and Exposition (ECCE), 2018, pp. 1233-1239, doi: 10.1109/ECCE.2018.8558063.

[10] R. Xie, Y. Shi, H. Li, “Study of 1200 V SiC JFET cascode device”, 2017 IEEE Workshop on Wide Bandgap Power Devices and Applications (WiPDA).

[11] Martin, Sandro, et al. "Comparative study of a 100kW PV WBG inverter using 1200V SiC MOSFET and JFET cascode devices." *2018 IEEE Applied Power Electronics Conference and Exposition (APEC)*. IEEE, 2018.

[12] Pellitteri, Filippo, et al. "Preliminary test on a cascode switch for high-frequency applications." 2020 2nd IEEE International Conference on Industrial Electronics for Sustainable Energy Systems (IESES). Vol. 1. IEEE, 2020.

[13] S. N. Agbo, E. Bashar, R. Wu, S. Mendy, J. O. Gonzalez and O. Alatise, "Simulations and Measurements of Failure Modes in SiC Cascode JFETs

under Short Circuit Conditions", *2021 IEEE 22nd Workshop on Control and Modelling of Power Electronics (COMPEL)*, pp. 1-7, 2021.

[14] B. Gao, A. Morgan, Y. Xu, X. Zhao, B. Ballard and D. C. Hopkins, "6.5 kv sic jfet-based super cascode power module with high avalanche energy handling capability", *2018 IEEE 6th Workshop on Wide Bandgap Power Devices and Applications (WiPDA)*, pp. 319-322, 2018.

[15] K. Katoh et al., "Study on low-loss gate drive circuit for high efficiency server power supply using normally-off SiC-JFET," 2014 International Power Electronics Conference (IPEC-Hiroshima 2014 - ECCE ASIA), Hiroshima, Japan, 2014, pp. 2285-2289, doi: 10.1109/IPEC.2014.6869908.

[16] X. Song and Y. Du, "Study of the SiC JFET Reverse Conduction and Reverse Blocking Characteristics," 2019 IEEE Applied Power Electronics Conference and Exposition (APEC), Anaheim, CA, USA, 2019, pp. 2751-2756, doi: 10.1109/APEC.2019.8721917.

[17] M. Caruso, A. O. Di Tommaso, F. Genduso and R. Miceli, "Experimental investigation on high efficiency real-time control algorithms for IPMSMs," 2014 International Conference on Renewable Energy Research and Application (ICRERA), Milwaukee, WI, USA, 2014, pp. 974-979.

[18] Caruso, M., et al. "Characterization of the parameters of interior permanent magnet synchronous motors for a loss model algorithm." Measurement 106 (2017): 196-202.

[19] V. Castiglia et al., "Modelling, Simulation and Characterization of a Supercapacitor in Automotive Applications," 2020 Fifteenth International Conference on Ecological Vehicles and Renewable Energies (EVER), Monte-Carlo, Monaco, 2020, pp. 1-6.

[20] V. Castiglia, P. Livreri, R. Miceli, F. Pellitteri, G. Schettino and F. Viola, "Power Management of a Battery/Supercapacitor System for E-Mobility Applications," 2019 AEIT International Conference of Electrical and Electronic Technologies for Automotive (AEIT AUTOMOTIVE), Turin, Italy, 2019, pp. 1-5.

[21] “Guidance for users of the CISPR Standards”, INTERNATIONAL SPECIAL COMMITTEE ON RADIO INTERFERENCE (CISPR). Available Online.